Diurnal Tide in the Equatorial Middle Atmosphere as Seen in LIMS Temperatures[1]

MATTHEW H. HITCHMAN AND CONWAY B. LEOVY

Department of Atmospheric Sciences, University of Washington, Seattle, WA 98195

(Manuscript received 16 July 1984, in final form 20 November 1984)

ABSTRACT

The distribution of day–night temperature differences in the middle atmosphere determined by the Nimbus 7 LIMS experiment is described. Day–night differences maximize at and are approximately symmetric about the equator. Successive centers of opposite sign increase in amplitude with altitude, the pattern having a vertical wavelength of ~25 km. Profiles of rocket meridional wind at Kwajalein (8.7°N) and Ascension Island (8.0°S) taken near local noon and averaged over the LIMS data period, exhibit maxima which support the tidal interpretation of the equatorial temperature pattern. These characteristics are in general agreement with previous observational and theoretical results for the solar driven diurnal tide. Substantial time variations in amplitude and in location of the temperature maxima are observed. The diurnal tide near the equatorial stratopause appears to be influenced by the phase of the semiannual oscillation.

1. Introduction

An observational description of the diurnal tide in the middle atmosphere has emerged chiefly through analyzing time series of rocket and radar profiles of wind and temperature. These data are generally of high vertical and temporal resolution, but sampling periods are usually short and the geographical coverage is sparse. Information of a complementary nature may be obtained from limb-scanning radiometers mounted on polar orbiting satellites. The LIMS instrument (Limb Infrared Monitor of the Stratosphere), active aboard the Nimbus 7 spacecraft during 25 October 1978–28 May 1979, yielded near-global coverage of high vertical resolution temperature profiles in the pressure range 100–0.05 mb. (~16–70 km). The satellite is in a sun-synchronous orbit, with the plane of the satellite's orbit always oriented parallel to the sun–earth axis. The LIMS instrument sampled the atmosphere near local noon on the ascending portion and near local midnight on the descending portion of each orbit. Because ascending–descending temperature differences are essentially day–night differences, they are expected to be representative of diurnal tide amplitudes. However, since the diurnal tide is also sun-synchronous, LIMS can only view the tide at two phases, unlike station profiles taken throughout the day.

Extended records of rocket meridional wind profiles taken near local noon at 8.7°N and 8.0°S provide another means of sampling the tide at a particular phase. A comparison with LIMS equatorial day–night temperature differences helps to verify the structure of the tide at low latitudes. Following a brief discussion of pertinent theory and of some past observations, the LIMS and rocket data are described. Then time mean and temporally varying aspects of LIMS ascending minus descending temperature differences are presented. Finally, low latitude LIMS, rocket, and model profiles are intercompared.

2. Theory and past observations

A comprehensive theoretical modeling study of the solar diurnal tide is given by Forbes (1982). The diurnal tide in the middle atmosphere is driven primarily by absorption of solar radiation by tropospheric water vapor and by ozone near the stratopause. Propagating modes that transmit energy away from the forcing region and have small vertical wavelengths dominate at low latitudes, while trapped evanescent modes having little phase tilt with height dominate at high latitudes. The most prominent mode in the middle atmosphere is expected to be the gravest symmetric propagating mode. Energy associated with this mode propagates upward from the thin region of strong water vapor heating in the troposphere, while phase propagates downward and migrates westward. For this mode temperature amplitudes reach a maximum at the equator, increasing exponentially with height until curtailed by dissipative effects in the upper mesosphere. This mode has a vertical wavelength of 25–30 km and, at a given level, a temperature perturbation of one sign at the equator is accompanied by weaker perturbations of the opposite sign near ±30° latitude.

In the vicinity of the equator, tidal meridional winds are due chiefly to acceleration down gradients of geopotential height. From hydrostatic considera-

[1] Contribution No. 709, Department of Atmospheric Sciences, University of Washington, Seattle, Washington.

tions, a descending warm center over the equator will be overlain by a center of high heights, in turn overlain by a cold center. Poleward acceleration will occur on the flanks of the descending center of high heights, with maximum poleward motion in the subtropics lagging maximum equatorial heights by ¼ cycle. Thus low equatorial temperatures are expected to be accompanied by subtropical poleward winds, high temperatures by equatorward winds.

The general transition of mode behavior from propagating at low latitudes to evanescent at high latitudes predicted by Lindzen (1967) has been verified by the rocket study of Reed *et al.*, (1969). However, above the stratopause at low latitude stations, observed vertical wavelengths were larger than predicted by theory. Reed *et al.* suggested that theory may be underestimating the strength of the *in situ* trapped tide generated by ozone heating near the stratopause. Improvements over Lindzen's model by Forbes (1982) include refinements in the distribution of forcing, Newtonian and mechanical damping, and, for all except the gravest mode, idealized background wind and temperature variations. Even so, some phase discrepancy persists above the stratopause.

Actual atmospheric conditions may be expected to differ from idealized theory or model results. Countryman and Dolas (1982) report coherent backscatter radar observations of tidal winds in the vertical range 62–86 km over Jicamarca, Peru (12°S, 77°W) during four 48-hour periods, one near each of the solstices and equinoxes. Departures from idealized tidal theory at this tropical station include day-to-day variability, reduced amplitude growth with height, and a standing-wave pattern for the equinox cases. Agreement with theoretically derived phases was poor in the lower mesosphere, near the region of local ozone forcing. They point out that strong vertical wind shear can produce reflection and interference. Thus day-to-day variability could be produced by wind shear variations. Day-to-day variability can also arise from changes in tropospheric water vapor amount at sub-global scales (Forbes and Groves, 1984). Such zonal asymmetries can force non-migrating, vertically propagating modes which have smaller vertical wavelengths than the dominant global migrating modes.

These factors can affect the dominant tidal pattern seen by LIMS. So can variations in local forcing, variations of strong thermal or mechanical damping, and variations in thermal stratification. Within the LIMS data record, one source of departure from an idealized steady background state at low latitudes is the semiannual oscillation of wind and temperature (SAO). Hirota (1980) gives a good review of observational aspects of the SAO.

3. Data

The LIMS experiment has been described by Gille and Russell (1984), and individual temperature retrievals have been compared with approximately contemporaneous and co-located rocket and radiosonde profiles, Gille *et al.*, (1984). The vertical resolution of temperature profiles is ~3 km and data accuracy is thought to be better than 2 K in the pressure range 100–1 mb. For a phenomenon with vertical wavelength ~ 25 km, amplitude reduction due to the finite vertical resolution is negligible (Gille *et al.*). Data used in this study are in the form of daily 1200 GMT synoptic grids of harmonic coefficients (13 coefficients: the zonal mean plus the sine and cosine coefficients of zonal waves 1–6) at 4 degree intervals from 64°S to 84°N and at 18 standard levels between 100 and 0.05 mb.

Mapped coefficients were calculated separately using values along the ascending portion (ascending coefficients), the descending portion (descending coefficients), and both portions (combined coefficients) of the orbit. As the earth turns beneath the satellite, the diurnal tide remains stationary with respect to the sun. Thus the ascending zonal mean coefficient is representative of the day side while the descending zonal mean coefficient is representative of the night side. Of course, the combined node zonal mean coefficient contains no tidal information.

Since the instrument looks back at an angle of 33.5° to the left of the orbit track, ascending-descending local time differences on a latitude circle depart from the ideal of 12 hours. This time interval is shortest near the poles, largest near 30°N and is 9.9 hours at the equator. Difference maxima would be reduced in amplitude by 3–13% in the latitude range 40°S–70°N due to sampling a diurnal sinusoidal wave at these shorter local time intervals (8.0–10.3 hours). At the equator, ascending–descending (1300–2300 local time) difference maxima are expected to underestimate noon–midnight difference maxima by only 8%.

An ambient temperature gradient along the line of sight can influence the relative amount of radiance received due to emission from CO_2 molecules at and above the tangent altitude. Thus ascending and descending temperature estimates can differ in a region of strong temperature gradient. This problem is minimal at the equator, where the thermal field is always nearly symmetric. Moreover, a "gradient correction" was implemented during inversion of the radiance profiles, in which first-guess temperatures were mapped, gradients estimated, and the inversion performed again using this information (Gille *et al.*, 1984). However, during periods of strong planetary wave activity at extra-tropical latitudes, gradient-induced differences are still noticeable at times. Gille *et al.* published a latitude–height section of ascending–descending differences for the limited period 1–12 January1979 but did not comment on possible tides.

LIMS mapped coefficients are not calculated where signal to noise is chronically poor. This often occurs at 100 and 0.05 mb, where the air is very cold. Regions of insufficient data are blank in the figures. To provide an accurate altitude scale, heights were constructed hydrostatically from time-mean LIMS temperatures. The scale appropriate at low latitudes appears on the right side of Figs. 2, 4 and 5, where the time-mean 100 mb surface occurs at an altitude of 16.5 km.

Rocket soundings of meridional wind at Kwajalein (8.7°N, and 167.7°E) and Ascension Island (8.0°S, 14.5°W) were obtained in computer tape format from the National Meteorological Data Center. Values used are at standard pressure levels, usually spanning 50–0.1 mb. Nestler (1983) describes the error characteristics of U.S. rocketsonde profiles. Above 50 km, temperature and wind data quality deteriorates due to decreasing air density. Temperatures are affected by decreased air to wire conduction and large aerodynamic heating, while rapid fall rates make sonde tracking and wind determination more difficult at these altitudes.

Nearly all of the rocket wind profiles were taken within three hours of 1300 local time, at roughly three-day intervals. The 80 Kwajalein soundings were distributed fairly evenly throughout the LIMS data record, with a gap during the second half of December. The 37 Ascension Island soundings were confined to the months January, February, April and May of 1979.

Theoretical phases and amplitudes for the diurnal tide are tabulated at every 6° of latitude and at roughly 5 km vertical spacing (Forbes and Gillette, 1982). For the temperature and wind comparisons that follow, their amplitudes and phases were interpolated to a 2 km vertical spacing. For temperature, equinox values at the equator were evaluated at local noon and midnight. For meridional wind, equinox values at 6°N, 12°N and 6°S, 12°S were interpolated to 9°N and 9°S, then evaluated at 1300 local time.

4. Results

The time mean latitude–height structure in LIMS ascending–descending temperature difference is shown in Fig. 1. In general agreement with theory for the diurnal tide, amplitudes maximize at the equator, increase upward, and a vertical wavelength of ~25 km is exhibited. Variation with time at the equator is shown in Fig. 2a. There is a broad modulation of amplitudes, with largest values centered in late February. As the amplitudes increase, positions of maxima and minima descend slightly. The daytime cold region near 0.5 mb is ~6 km lower in February than in December. Time mean amplitudes in Fig. 1 are smaller than typical daily values because they are smeared out by this phase variability.

The latitudinal position of the daytime cold maximum at 0.5 mb varies with time as shown in Fig. 3.

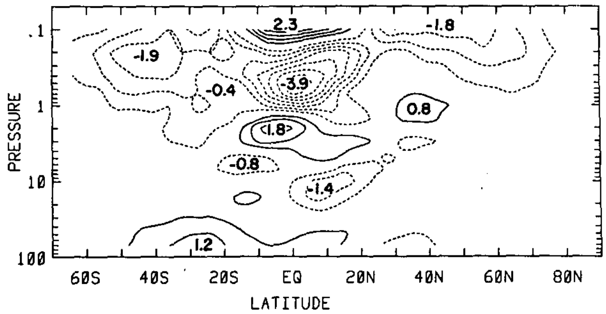

FIG. 1. Latitude–height section of LIMS ascending minus descending zonal mean temperature, averaged for the 216-day record. The contour interval is 0.5 K. The zero contour has been omitted for clarity.

It lies somewhat north of the equator during January and February and somewhat south of it during May. There is also evidence for flanking daytime warm regions near 20°S and 30°N when the equatorial signal is strong. The noisy features at extra-tropical latitudes are probably due to incomplete removal of radiance gradient errors associated with planetary wave activity.

The time mean profile of LIMS ascending–descending temperature at the equator is compared with theory and some previous rocket results in Fig. 4. Finger *et al.* (1975) reported a favorable comparison between Lindzen's theoretical curve for the diurnal tide at the equator and day–night rocket temperature profiles taken at the French Guiana Space Center (5°N, 52°W) during 20 September–1 October 1973. In that study approximately six daytime and six nighttime profiles, within 3 hours of local noon or midnight, were taken by each of French, U.K., U.S.S.R., and U.S. rocketsondes, and day–night differences were averaged for each country. An estimated average of those four profiles, together with Lindzen's theoretical curve, are taken from their Fig. 9 and reproduced here in Fig. 4. Also shown in Fig. 4 is Forbes' updated theoretical curve. A characteristic vertical wavelength of 25–30 km is seen in all four curves.

If 12 hour differences are taken for time pairs other than local noon–midnght, the vertical positions of the maxima would be different. One may imagine two envelope curves drawn tangent to the negative and positive maxima for a given profile in Fig. 4. These envelopes would be tangent to the maxima for all 12 hour time pairs through one tidal period and would provide an estimate of temperature amplitude as a function of altitude. The LIMS and rocket profiles do not represent exact 12 hour differences. For the LIMS data on the equator an amplitude reduction of only 8% is expected due to the shorter actual sampling time interval. Similarly, vertical positions of the LIMS maxima may be expected to

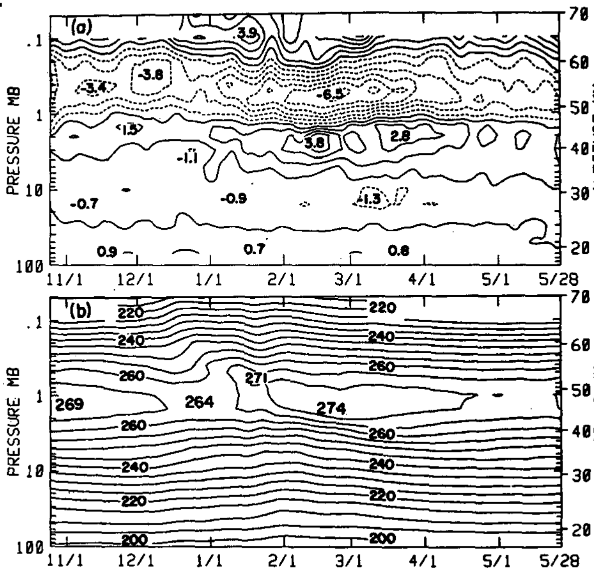

FIG. 2. Time-height sections of (a) LIMS ascending minus descending temperature (contour interval 0.5 K) and (b) LIMS combined temperature (contour interval 5 K) near the equator. Averages of zonal mean coefficients at 4°S, 0°, and 4°N are used. Daily values have been smoothed in time with a 1-2-1 filter.

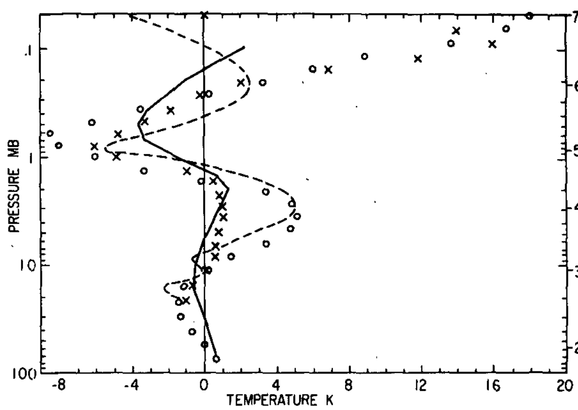

FIG. 4. Time mean profile of LIMS ascending minus descending temperature using the average of zonal mean coefficients at 4°S, 0°, and 4°N (solid curve), estimated average day-night rocket profile of Finger *et al.* (dashed curve), Lindzen's original model results (crosses), and Forbes' improved model results (circles) at the equator (see text). Time variations of phase are partly responsible for the relatively small LIMS time mean amplitudes.

depart from noon-midnight positions by less than 2 km.

Time mean LIMS amplitudes are smaller than shown by either the rocket data, which were collected over a period of only 10 days, or the theoretical results, which have no day-to-day phase variation. As suggested by Figs. 1–3, this is primarily due to averaging LIMS profiles which exhibit temporal trends in vertical positions of the maxima. Note that in February (Fig. 2a) LIMS amplitudes are quite similar to both the theoretical and the rocket values. The locations of the LIMS maxima near 43 km and 30 km in the time mean profile are also at lower altitudes in February, in better agreement with the other curves. Above 60 km, LIMS data suggest a positive trend with height which is not as strong as the theory predicts, while the rocket data show the opposite trend. However, both LIMS and rocket data have decreasing accuracy at these higher altitudes.

Figure 5 shows that there is good agreement between theory and long time series of rocket daytime meridional winds. Because Kwajalein and Ascension Island are located in opposite hemispheres, local noon winds should have the opposite sign. Bearing in mind the relationship between temperature and meridional wind expected from theory, these wind profiles gen-

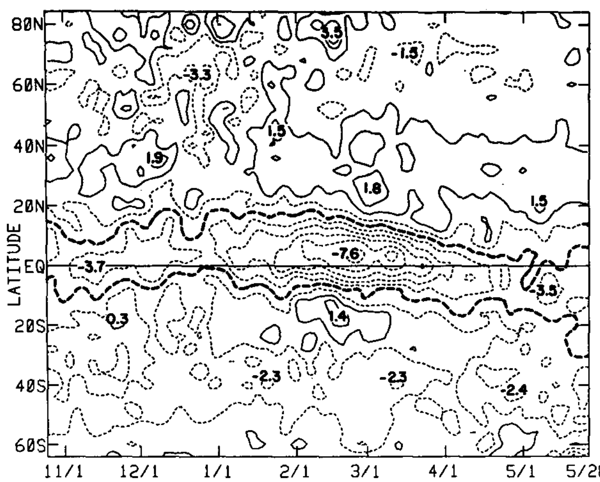

FIG. 3. Time-latitude section of LIMS ascending minus descending zonal mean temperature at 0.5 mb. The contour interval is 1 K. The −2 K contour is emphasized by thick dashes. Daily values have been smoothed in time with a 1-2-1 filter.

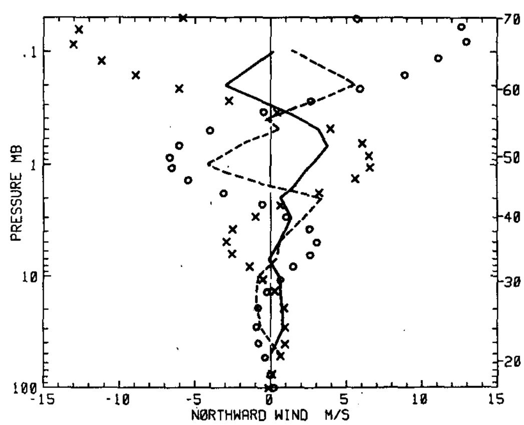

FIG. 5. Time mean profiles of rocket meridional wind taken near local noon at Kwajalein (8.7°N) (solid curve) and Ascension Island (8.0°S) (dashed curve), together with Forbes' model results interpolated to 9°N (crosses) and 9°S (circles), (see text). Time variations of phase are partly responsible for the relatively small rocket time mean amplitudes.

erally verify the vertical locations as well as the amplitudes of the temperature maxima. Near 25 and 50 km the daytime cold regions are flanked by poleward motion. The equatorward motion expected near 36 km occurs at a higher altitude at Ascension Island and is apparently absent at Kwajalein. Again, rocket amplitudes are reduced by time averaging over these 7 months during which substantial phase variations occur. Moreover, any steady nontidal meridional wind components at the longitudes of these stations would bias the profiles. Above 60 km the discrepancy with theory may be due to rocket error.

All of the figures suggest that the diurnal tide is rather complex and that departures from idealized theoretical results occur. Temporal variations seen in Figs. 2a and 3 may be related to changes in the background mean state caused by the SAO. A time-height section of zonal mean wind at the equator is presented by Hitchman (1985). Stratopause level winds range from −40 to 30 m s^{-1} in association with the SAO. 15% variations in LIMS derived ozone occur at stratopause levels (not shown) in connection with SAO temperature variations of ~10 K. Of the three parameters ozone, zonal wind, and temperature, changes in the daily mean temperature field (Fig. 2b) seem to correlate best with the changes in ascending–descending temperature differences (Fig. 2a). The SAO warm region descends from near 70 km in December to 50 km by February, sharpening the stratopause. The stratopause is weak in late December due to the SAO cold region present at that time. The intensification of the tidal signal from December through February corresponds well with this sharpening of the mean stratopause in association with the equatorial SAO. This tends to substantiate the mode distortion hypothesis (Lindzen 1972; Forbes 1982), in which the propagating modes are affected by the background state, although detailed theoretical calculations are needed to verify the relationship suggested by Fig. 2. Trends in local ozone forcing and water vapor forcing probably also contribute to the observed changes.

Acknowledgments. We are grateful to Dr. Forbes for providing us with the manuscript containing his tabulated model results. We would also like to thank Dr. Ellis Remsberg for helpful discussions and Nancy Wytko for typing the manuscript. This work was supported by NASA under Grant NAGW471.

REFERENCES

Countryman, I. D., and P. M. Dolas, 1982: Observations on tides in the equatorial mesosphere. *J. Geophys. Res.*, **87**(C2), 1336–1342.

Finger, F. G., M. E. Gelman, F. J. Schmidlin, R. Leviton and V. W. Kennedy, 1975: Compatibility of meteorological rocketsonde data as indicated by international comparison tests. *J. Atmos. Sci.*, **32**, 1705–1714.

Forbes, J. M., 1982: Atmospheric tides 1. Model description and results for the solar diurnal component. *J. Geophys. Res.*, **87**(A7), 5222–5240.

——, and D. F. Gillette, 1982: A compendium of theoretical atmospheric tidal structures. Part 1: Model description and explicit structures due to realistic thermal and gravitational excitation. Air Force Geophysics Laboratory, Environ. Res. Paper No. 780(I). [NTIS Order No. AD-A125 720/3.]

——, and G. V. Groves, 1985: Diurnal propagating tides in the low latitude middle atmosphere. Submitted to *J. Atmos. Terr. Phys.*

Gille, J. C., and J. M. Russell III, 1984: The Limb Infrared Monitor of the Stratosphere (LIMS) experiment description, performance, and results. *J. Geophys. Res.*, **89**(D4), 5125–5140.

——, ——, P. L. Bailey, L. L. Gordley, E. e. Remsberg, J. H. Leinesch, W. G. Planet, F. B. House, L. V. Lyjak and S. A. Beck, 1984: Validation of temperature retrievals obtained by the Limb Infrared Monitor of the Stratosphere (LIMS) experiment on Nimbus 7. *J. Geophys. Res.*, **89**(D4), 5147–5160.

Hirota, I., 1980: Observational evidence of the semiannual oscillation in the tropical middle atmosphere—a review. *Pure Appl. Geophys.* **118**, 217–238.

Hitchman, M. H., 1985: An observational study of wave–mean flow interaction in the equatorial middle atmosphere. Ph.D. dissertation, University of Washingtion, 360 pp.

Lindzen, R. S., 1967: Thermally driven diurnal tide in the atmosphere. *Quart. J. Roy. Meteor. Soc.*, **93**, 18–42.

——, 1972: Equatorial planetary waves in shear: Part II. *J. Atmos. Sci.*, **29**, 1452–1463.

Nestler, M. S., 1983: A comparative study of measurements from radiosondes, rocketsondes, and satellites. NASA Contractor Report 168343.

Reed, R. J., M. J. Oard and M. Sieminski, 1969: A comparison of observed and theoretical diurnal tidal motions between 30 and 60 kilometers. *Mon. Wea. Rev.*, **97**, 456–459.